

Chiral symmetry restoration versus deconfinement in heavy-ion collisions at high baryon density

W. Cassing,¹ A. Palmese,¹ P. Moreau,^{2,3} and E. L. Bratkovskaya^{2,3}

¹*Institut für Theoretische Physik, Universität Gießen, Germany*

²*Frankfurt Institute for Advanced Studies, Johann Wolfgang Goethe Universität, Frankfurt am Main, Germany*

³*Institute for Theoretical Physics, Johann Wolfgang Goethe Universität, Frankfurt am Main, Germany*

We study the production of strange hadrons in nucleus-nucleus collisions from 4 to 160 A GeV within the Parton-Hadron-String Dynamics (PHSD) transport approach that is extended to incorporate essential aspects of chiral symmetry restoration (CSR) in the hadronic sector (via the Schwinger mechanism) on top of the deconfinement phase transition as implemented in PHSD. Especially the K^+/π^+ and the $(\Lambda + \Sigma^0)/\pi^-$ ratios in central Au+Au collisions are found to provide information on the relative importance of both transitions. The modelling of chiral symmetry restoration is driven by the pion-nucleon Σ -term in the computation of the quark scalar condensate $\langle q\bar{q} \rangle$ that serves as an order parameter for CSR and also scales approximately with the effective quark masses m_s and m_q . Furthermore, the nucleon scalar density ρ_s , which also enters the computation of $\langle q\bar{q} \rangle$, is evaluated within the nonlinear $\sigma - \omega$ model which is constraint by Dirac-Brueckner calculations and low energy heavy-ion reactions. The Schwinger mechanism (for string decay) fixes the ratio of strange to light quark production in the hadronic medium. We find that above ~ 80 A GeV the reaction dynamics of heavy nuclei is dominantly driven by partonic degrees-of-freedom such that traces of the chiral symmetry restoration are hard to identify. Our studies support the conjecture of 'quarkyonic matter' in heavy-ion collisions from about 5 to 40 A GeV and provide a microscopic explanation for the maximum in the K^+/π^+ ratio at about 30 A GeV which only shows up if a transition to partonic degrees-of-freedom is incorporated in the reaction dynamics and is discarded in the traditional hadron-string models.

PACS numbers: 25.75.Nq, 25.75.Ld, 25.75.-q, 24.85.+p, 12.38.Mh

I. INTRODUCTION

According to Quantum Chromo Dynamics (QCD) [1–6], matter changes its phase at high temperature and density and bound (colorless) hadrons dissolve to interacting (colored) quarks and gluons in the Quark-Gluon-Plasma (QGP). Along with this deconfinement phase transition at low quark chemical potential μ_q a restoration of chiral symmetry (CSR) is observed in lattice QCD (lQCD) calculations at roughly the same critical temperature or energy density. Since at low μ_q the phase change is a crossover both transitions do not (have to) occur at the same temperature. The study of the phase boundaries and the properties of the QGP are the main goal of several present and future heavy-ion experiments at SPS (Super Proton Synchrotron), RHIC (Relativistic Heavy-Ion Collider), LHC (Large Hadron Collider) and the future FAIR (Facility for Antiproton and Ion Research) as well as NICA (Nuclotron-based Ion Collider fAcility) [7]. Since the QGP is created only for a short time (of a couple of fm/c) it is quite demanding to study its properties and to find sensible probes for chiral symmetry restoration as well as for the deconfinement transition. Only by the measurement of the 'bulk' light hadrons, electromagnetic probes (dileptons and photons), heavy mesons, jets and related correlations we might be able to disentangle the different physics at the phase boundaries especially at high quark chemical potential μ_q where a first order transition might take place [8–11].

The question of chiral symmetry restoration at high

baryon density and/or high temperature is of fundamental interest in itself and dilepton studies in nucleus-nucleus collisions have been driven by the notion to find signatures for a CSR. As noted above the situation is less clear for finite baryon density where QCD sum rule studies indicate a linear decrease of the scalar quark condensate $\langle \bar{q}q \rangle$ – which is nonvanishing in the vacuum due to a spontaneous breaking of chiral symmetry – with baryon density ρ_B towards a chiral symmetric phase characterized by $\langle \bar{q}q \rangle \approx 0$ [12, 13]. This decrease of the scalar quark condensate is expected to lead to a change of the hadron properties with density and temperature, i.e. in a chirally restored phase the vector and axial vector currents should become equal [14–18]; the latter implies that e.g. the ρ and a_1 spectral functions should become identical. Since the scalar quark condensate $\langle \bar{q}q \rangle$ is not a direct observable, its manifestations should be found indirectly in different hadronic abundancies and spectra or particle ratios like K^+/π^+ , $(\Lambda + \Sigma^0)/\pi^-$ etc.

Nowadays, our knowledge about the hadron properties at high temperature or baryon density is based on heavy-ion experiments from SchwerIonen-Synchrotron (SIS) to SPS energies where hot and dense nuclear systems are produced on a timescale of a few fm/c together with partonic subsystems. The information from ultra-relativistic nucleus-nucleus collisions at RHIC or LHC essentially addresses the dominant partonic phases at low quark chemical potential μ_q , a region which can be well addressed by lQCD, too. This knowledge, however, does not allow for proper extrapolations to the properties of QCD

at high baryon density which has been the major motivation for the future construction of the FAIR/NICA facilities and is in the focus of the Beam-Energy-Scan (BES) program at RHIC. However, any informations on the properties of hadrons in the nuclear environment are obtained from the comparison of experimental data with nonequilibrium kinetic transport theory [19–27]. As a genuine feature of transport theories in the hadronic sector there are two essential ingredients: i.e. the *baryon (and meson) scalar and vector self-energies* as well as *in-medium elastic and inelastic cross sections* (or transition matrix elements) for all hadrons involved. Whereas in the low-energy regime these ‘transport coefficients’ can be calculated in the Dirac-Brueckner approach starting from the bare nucleon-nucleon interaction [28–32] this is no longer possible at high baryon density ($\rho_B \geq 2\text{--}3\rho_0$) and high temperature, since the number of independent hadronic degrees-of-freedom increases drastically and the interacting hadronic system should approach a phase with $\langle q\bar{q} \rangle \approx 0$ [12, 14, 16, 17] as mentioned before.

In this work we will concentrate on excitation functions of hadronic observables from SIS to SPS energies with the aim to find out optimal experimental conditions to search for ‘traditional’ phenomena such as strangeness enhancement in nucleus-nucleus collisions [33, 34] or the ‘horn’ in the K^+/π^+ ratio [35, 36]. Both phenomena have been addressed to a deconfinement transition. Indeed, the actual experimental observation could not be described within conventional hadronic transport theory [37–39] and remained a major challenge for microscopic approaches. Only within hybrid approaches [40] or three-fluid hydrodynamics [41] a description of the ‘horn phenomenon’ could be achieved due to the assumption of chemical equilibrium in the hydro phase. This also holds true for the statistical model fits assuming full chemical equilibration [42]. However, hadronic interaction rates showed up to be too slow to reach chemical equilibrium in these nucleus-nucleus collisions [43]. This was also found for the partonic stage in Ref. [44]. Accordingly, the quest for a microscopic explanation of the K^+/π^+ ‘horn’ remained.

In 2006 McLerran and Pisarski suggested that a new form of matter might exist at high baryon chemical potential [45] where the degrees-of-freedom are still confined but chiral symmetry is restored such that parity doublets appear in the excitation spectrum. This lead to an extended scenario for the phase diagram of strongly interacting matter [46, 47]. Although a clear separated phase of such ‘quarkyonic matter’ might be overtaken one could expect a partially chiral restored phase before deconfinement sets in as suggested also by Nambu-Jona-Lasinio models [48–51].

Our studies are performed within the PHSD transport approach that has been described in Refs. [52, 53]. PHSD incorporates explicit partonic degrees-of-freedom in terms of strongly interacting quasiparticles (quarks and gluons) in line with an equation-of-state from lattice QCD (lQCD) as well as dynamical hadronization

and hadronic elastic and inelastic collisions in the final reaction phase. This approach has been tested for $p + p$, $p + A$ and $A + A$ collisions from the SPS to LHC energy regime [52–55]. We recall that longitudinal and transverse momentum spectra of nucleons, pions, kaons and antibaryons have been successfully reproduced within PHSD within the full energy range from the upper SPS to LHC energies as well dilepton and photon observables. Moreover, the collective flow coefficients v_n for the azimuthal angular distributions were found to be well in line with the PHSD calculations as well as the suppression of hard probes such as charm quarks at RHIC energies [56]. However, in all these studies the question of chiral symmetry restoration has been discarded since the observables analyzed were driven by the dominant deconfinement transition and the parton dynamics in the QGP. Only when going down in bombarding energy to the Alternating-Gradient-Synchrotron (AGS) regime severe discrepancies were found [57] in the directed proton, pion and kaon flows as well as in the strangeness production. The actual results at AGS energies are close to those from the Hadron-String Dynamics (HSD) transport approach (without a partonic phase) in Refs. [38, 39, 58]. This does not come as a surprise since at low energy densities ($\epsilon < 0.5 \text{ GeV}/\text{fm}^3$) the PHSD merges with HSD. By observing that the discrepancies show up already within HSD - and are very similar in PHSD - we conclude that the deconfinement phase transition does not show ‘responsibility’ for these discrepancies.

We here suggest that the missing ‘strangeness’ is due to the neglect of chiral symmetry restoration (in the Schwinger mechanism of string decay) at high baryon density. Accordingly, a partial restoration of chiral symmetry may be achieved in the hadronic but confined phase. Such a situation might be attributed to ‘quarkyonic matter’ out-of-equilibrium. To investigate this proposal we extend the existing PHSD transport approach [52] to include essential facets of chiral symmetry restoration in terms of the Schwinger mechanism for string decay. Since PHSD has been successfully applied to describe the final distribution of mesons (with light quark content) from SPS up to LHC energies [52–55], it provides a solid framework for the description of the creation, expansion and hadronization of the QGP as well as the hadronic expansion with partly resonant scatterings (like $\pi + N \leftrightarrow \Delta$ or $\pi + \pi \leftrightarrow \rho$).

This study is organized as follows: In Sec. II we recall the basic ideas of the PHSD approach and describe the evaluation of the scalar quark condensate as well as the modified string decay in line with CSR. Sec. III is devoted to the actual computation of particle spectra and particle ratios in central Au+Au collisions from 4 to 158 A GeV in different limits, i.e. with and without CSR, with and without partonic degrees-of-freedom. A summary completes this work in Sec. IV.

II. THE PHSD TRANSPORT APPROACH

A. Basic concepts

The Parton-Hadron-String Dynamics (PHSD) transport approach [52, 53] is a microscopic covariant dynamical model for strongly interacting systems formulated on the basis of Kadanoff-Baym equations [59–61] for Green's functions in phase-space representation (in first order gradient expansion beyond the quasiparticle approximation). The approach consistently describes the full evolution of a relativistic heavy-ion collision from the initial hard scatterings and string formation through the dynamical deconfinement phase transition to the strongly-interacting quark-gluon plasma (sQGP) as well as hadronization and the subsequent interactions in the expanding hadronic phase as in the Hadron-String-Dynamics (HSD) transport approach [23]. The transport theoretical description of quarks and gluons in the PHSD is based on the Dynamical Quasi-Particle Model (DQPM) for partons that is constructed to reproduce IQCD results for a quark-gluon plasma in thermodynamic equilibrium [61] on the basis of effective propagators for quarks and gluons. The DQPM is thermodynamically consistent and the effective parton propagators incorporate finite masses (scalar mean-fields) for gluons/quarks as well as a finite width that describes the medium dependent reaction rate. For fixed thermodynamic temperature T the partonic widths $\Gamma_i(T)$ fix the effective two-body interactions that are presently implemented in the PHSD [44]. The PHSD differs from conventional Boltzmann approaches in a couple of essential aspects:

- it incorporates dynamical quasi-particles due to the finite width of the spectral functions (imaginary part of the propagators) in line with complex retarded selfenergies;
- it involves scalar mean-fields that substantially drive the collective flow in the partonic phase;
- it is based on a realistic equation of state from lattice QCD and thus reproduces the speed of sound $c_s(T)$ reliably;
- the hadronization is described by the fusion of off-shell partons to off-shell hadronic states (resonances or strings);
- all conservation laws (energy-momentum, flavor currents etc.) are fulfilled in the hadronization contrary to coalescence models;
- the effective partonic cross sections no longer are given by pQCD and are 'defined' by the DQPM in a consistent fashion. These cross sections are probed by transport coefficients (correlators) in thermodynamic equilibrium by performing PHSD calculations in a finite box with periodic boundary conditions (shear- and bulk viscosity, electric conductivity, magnetic susceptibility etc. [62, 63]).

An actual nucleus-nucleus collision within PHSD proceeds as follows: in the beginning of a relativistic heavy-ion collisions color-neutral strings (described by the FRITIOF LUND model [64]) (including PYTHIA 6.4 [65]) are produced in hard scatterings of nucleons from the impinging nuclei. These strings are dissolved into 'pre-hadrons' with a formation time of ~ 0.8 fm/c in their rest frame, except for the 'leading hadrons', i.e. the fastest residues of the string ends, which can re-interact (practically instantly) with hadrons with a reduced cross sections in line with quark counting rules. If, however, the local energy density is larger than the critical value for the phase transition, which is taken to be ~ 0.5 GeV/fm³ in line with IQCD [3], the pre-hadrons melt into (colored) effective quarks and antiquarks in their self-generated repulsive mean-field as defined by the DQPM [61]. In the DQPM the quarks, antiquarks and gluons are dressed quasiparticles and have temperature-dependent effective masses and widths which have been fitted to lattice thermal quantities such as energy density, pressure and entropy density. The nonzero width of the quasiparticles implies the off-shellness of partons, which is taken into account in the scattering and propagation of partons in the QGP on the same footing (i.e. propagators and couplings).

The transition from the partonic to hadronic degrees-of-freedom (for light quarks/antiquarks) is described by covariant transition rates for the fusion of quark-antiquark pairs to mesonic resonances or three quarks (antiquarks) to baryonic states, i.e. by the dynamical hadronization. We already mention here that this hadronization process is restricted to 'bulk' transverse momenta p_T up to ~ 2 GeV and has to be replaced by fragmentation for high p_T [56] in future. Note that due to the off-shell nature of both partons and hadrons, the hadronization process described above obeys all conservation laws (i.e. four-momentum conservation and flavor current conservation) in each event, the detailed balance relations and the increase in the total entropy S .

In the hadronic phase PHSD is equivalent to the hadron-strings dynamics (HSD) model [23] that has been employed in the past from SIS to SPS energies. On the other hand the PHSD approach has been tested for p+p, p+A and relativistic heavy-ion collisions from lower SPS to LHC energies and been successful in describing a large number of experimental data including single-particle spectra, collective flow [52–54, 66] as well as electromagnetic probes [55] or charm observables [56].

B. Strings in (P)HSD

In the PHSD/HSD the string excitation and decay plays a decisive role for elastic and inelastic collisions which has been well tested for hadronic reactions in vacuum in a wide energy range. We recall that in the hadronic phase the high energy inelastic hadron-hadron collisions are described by the FRITIOF model [64],

where two incoming nucleons emerge the reaction as two excited color singlet states, i.e. 'strings'. According to the FRITIOF model a string is characterized by the leading constituent quarks of the incoming hadron and a tube of color flux is supposed to be formed connecting the rapidly receding string-ends. In the PHSD approach baryonic ($qq - q$) and mesonic ($q - \bar{q}$) strings are considered with different flavors ($q = u, d, s$). In the uniform color field of the strings virtual $q\bar{q}$ or $qq\bar{q}\bar{q}$ pairs are produced causing the tube to fission and thus to create mesons or baryon-antibaryon pairs (with a formation time ~ 0.8 fm/c). The production probability P of massive $s\bar{s}$ or $qq\bar{q}\bar{q}$ pairs is suppressed in comparison to light flavor production ($u\bar{u}$, $d\bar{d}$) according to a Schwinger-like formula [67], i.e.

$$\frac{P(s\bar{s})}{P(u\bar{u})} = \frac{P(s\bar{s})}{P(d\bar{d})} = \gamma_s = \exp\left(-\pi \frac{m_s^2 - m_q^2}{2\kappa}\right), \quad (1)$$

with $\kappa \approx 0.176$ GeV² denoting the string tension and $m_s, m_q = m_u = m_d$ the appropriate strange and light quark masses. Thus in the Lund string picture the production of strangeness and baryon-antibaryon pairs is controlled by the constituent quark (and diquark) masses. Inserting the constituent (dressed) quark masses $m_u \approx 0.33$ GeV and $m_s \approx 0.5$ GeV in the vacuum a value of $\gamma_s \approx 0.3$ is obtained from Eq. (1). While the strangeness production in proton-proton collisions at SPS energies is reasonably well reproduced with this value, the strangeness yield for p + Be collisions at AGS energies is underestimated by roughly 30% (cf. [37]). For that reason the relative factors used in the PHSD/HSD model are [37]

$$u : d : s : uu = \begin{cases} 1 : 1 : 0.3 : 0.07 & , \text{at SPS to RHIC} \\ 1 : 1 : 0.4 : 0.07 & , \text{at AGS energies,} \end{cases} \quad (2)$$

with a linear transition of the strangeness suppression factor γ_s as a function of \sqrt{s} in between. These settings have been fixed in Ref. [37] for HSD in 1998 and kept since then also for PHSD.

Additionally a fragmentation function $f(x, m_t)$ has to be specified, which is the probability distribution for hadrons with transverse mass m_T to acquire the energy-momentum fraction x from the fragmenting string,

$$f(x, m_T) \approx \frac{1}{x} (1-x)^a \exp(-bm_T^2/x), \quad (3)$$

with $a = 0.23$ and $b = 0.34$ GeV⁻² [37]. These settings for the string decay to hadrons have been found to match well experimental observations for particle production in p+p and p+A reactions [23]. In these reactions the vacuum constituent (dressed) quark masses m_s and m_q are relevant that, however, should be different in the nuclear medium as noted above. We mention that in HSD/PHSD we include antinucleon annihilation into several mesons while taking into account also the inverse processes of $N\bar{N}$ creation in multi-meson interactions by detailed balance [68].

C. Extensions in PHSD with respect to HSD2.3

The modifications in PHSD3.3 with respect to the HSD version 2.3 from 2003 employed in the previous studies in Refs. [38, 39] are as follows:

- The energy-density cut for hadronic interactions ($\epsilon_c \leq 1$ GeV/fm³) has been reduced to $\epsilon_c \leq 0.5$ GeV/fm³ because the unquenched lattice QCD results from the BMW Collaboration in 2009 [2] were converging to the lower critical energy density $\epsilon_c \approx 0.5$ GeV/fm³ for the deconfinement phase transition. Accordingly, inelastic hadronic collisions in local cells with energy density $0.5 \text{ GeV/fm}^3 \leq \epsilon \leq 1 \text{ GeV/fm}^3$ no longer happen in the actual version which leads to a reduction of the meson multiplicity (dominantly pions and kaons) by about 10 to 15%. Since kaons and pions are effected by about the same reduction factor their ratios practically do not change.
- The inverse processes of $N\bar{N}$ creation in multi-meson interactions by detailed balance [68] are now included by default.
- A couple of strangeness exchange reactions have been added in meson-baryon and baryon-baryon collisions following Refs. [69–71].
- The hadronic reaction channels are symmetric now with respect to $m + B \leftrightarrow \bar{m} + \bar{B}$. This has a minor impact at the laboratory energies considered in this study.

After reviewing the basic concepts of the PHSD approach we now come to the modeling of chiral symmetry restoration in the PHSD.

D. The scalar quark condensate

As is well known the scalar quark condensate $\langle q\bar{q} \rangle$ is viewed as an order parameter for the restoration of chiral symmetry at high baryon density and temperature, however, it is not a quantity that can directly be determined by experiment. Nevertheless, some close links to low energy constants and nuclear quantities can be employed to determine the scalar quark condensate.

A reasonable estimate for the quark scalar condensate in dynamical calculations has been suggested by Friman et al. [74],

$$\frac{\langle q\bar{q} \rangle}{\langle q\bar{q} \rangle_V} = 1 - \frac{\Sigma_\pi}{f_\pi^2 m_\pi^2} \rho_S - \sum_h \frac{\sigma_h \rho_S^h}{f_\pi^2 m_\pi^2}, \quad (4)$$

where σ_h denotes the σ -commutator of the relevant mesons h . Furthermore, $\langle q\bar{q} \rangle_V$ denotes the vacuum condensate, $\Sigma_\pi \approx 45$ MeV is the pion-nucleon Σ -term, f_π and m_π the pion decay constant and pion mass, respectively. Since for low densities the scalar density ρ_S in (4)

may be replaced by the baryon density ρ_B , the change in the scalar quark condensate starts linearly with ρ_B and is reduced by a factor $\approx 1/3$ at saturation density $\rho_0 \approx 1/6 \text{ fm}^{-3}$. Note, however, that the value of Σ_π is not so accurately known; a recent analysis points towards a larger value of $\Sigma_\pi \approx 59 \text{ MeV}$ [72] while actual IQCD results [73] suggest a slightly lower value. Accordingly, our following calculations - based on $\Sigma_\pi = 45 \text{ MeV}$ - have to be taken with some care.

For pions and mesons made out of light quarks and antiquarks we use $\sigma_h = m_\pi/2$ [73] whereas for mesons with a strange (antistrange) quark we adopt $\sigma_h = m_\pi/4$ according to the light quark content. Within the same spirit the σ -term for hyperons is taken as $2/3 \Sigma_\pi \approx 30 \text{ MeV}$ while for Ξ 's we use $1/3 \Sigma_\pi \approx 15 \text{ MeV}$. The vacuum scalar condensate $\langle q\bar{q} \rangle_V$ is fixed by the Gell-Mann-Oakes-Renner (GOR) relation [75, 76]

$$f_\pi^2 m_\pi^2 = -\frac{1}{2}(m_u^0 + m_d^0) \langle q\bar{q} \rangle_V \quad (5)$$

to $\langle q\bar{q} \rangle_V \approx -1.6 \text{ fm}^{-3}$ for the bare quark masses $m_u^0 = m_d^0 \approx 7 \text{ MeV}$. The scalar density of mesons (of type h) in (4) is given by ($x = (\mathbf{r}, t)$)

$$\rho_S^h(x) = \frac{(2s+1)(2t+1)}{(2\pi)^3} \int d^3\mathbf{p} \frac{m_h}{\sqrt{\mathbf{p}^2 + m_h^2}} f_h(x, \mathbf{p}), \quad (6)$$

with $f_h(x, \mathbf{p})$ denoting the meson phase-space distribution of species h . In (6) s, t denote the discrete spin and isospin quantum numbers, respectively. The last quantity in the relation (4), that still has to be determined for an evaluation of the quark condensate, is the nucleon scalar density ρ_S .

E. The nuclear scalar density

The scalar density of nucleons ρ_S can be calculated in line with (6) by replacing the mass and momentum by the effective quantities

$$m_N^*(x) = m_N^v - g_s \sigma(x) \quad (7)$$

with m_N^v denoting the nucleon mass in vacuum. In Eq. (7) the scalar field $\sigma(x)$ mediates the scalar interaction with the surrounding medium while g_s is a coupling. When including self-interactions of the σ -field up to 4th order [77] the scalar field is determined locally by the nonlinear gap equation [77, 78]

$$\begin{aligned} m_s^2 \sigma(x) + B\sigma^2(x) + C\sigma^3(x) &= g_s \rho_S \quad (8) \\ &= g_s d \int \frac{d^3p}{(2\pi)^3} \frac{m_N^*(x)}{\sqrt{p^2 + m_N^{*2}}} f_N(x, \mathbf{p}) \end{aligned}$$

with $d = 4$ in case of isospin symmetric nuclear matter. The parameters g_s, m_s, B, C are fixed in the non-linear

	NL1	ML2	NL3
g_s	6.91	9.28	9.50
g_v	7.54	10.59	10.95
B (1/fm)	-40.6	5.1	1.589
C	384.4	9.8	34.23
m_s (1/fm)	2.79	2.79	2.79
m_v (1/fm)	3.97	3.97	3.97
K (MeV)	380	354	380
m^*/m	0.83	0.68	0.70

TABLE I. Parameter sets NL1, ML2 and NL3 for the nonlinear $\sigma - \omega$ model employed in the transport calculations [78].

$\sigma - \omega$ model for nuclear matter [78] and are displayed in Table I specifying also the vector coupling g_v and vector meson mass m_v . We will use the NL3 set in the following with a compressibility $K = 380 \text{ MeV}$ and effective mass $m^*/m = 0.7$ at normal nuclear matter density. In order to obtain an estimate on the uncertainties of our results we have also used the sets NL1 and ML2. We recall that in the non-linear $\sigma - \omega$ model the energy density for symmetric nuclear matter is given by [78]

$$\epsilon = U(\sigma) + \frac{g_v^2}{2m_v^2} \rho_N^2 + d \int \frac{d^3p}{(2\pi)^3} E^*(\mathbf{p}) (N_c(\mathbf{p}) + N_d(\mathbf{p})), \quad (9)$$

with

$$E^*(\mathbf{p}) = \sqrt{\mathbf{p}^2 + m_B^{*2}},$$

$$U(\sigma) = \frac{m_s^2}{2} \sigma^2 + \frac{B}{3} \sigma^3 + \frac{C}{4} \sigma^4$$

while ρ_N denotes the baryon density and $N_c(\mathbf{p})$ and $N_d(\mathbf{p})$ the particle/antiparticle numbers at fixed momentum \mathbf{p} .

Actual results for the effective nucleon mass (divided by the vacuum mass) at temperature $T = 0$ are displayed in Fig. 1 by the dashed (blue) line (for NL3) as a function of the energy density ϵ given by Eq. (9). We find an almost linear decrease of the effective nucleon mass with energy density with a slope that essentially scales with the effective mass m_N^*/m_N^v at normal nuclear matter density ρ_0 (cf. Table I). Since for $T = 0$ there are no thermal mesons the resulting ratio for the scalar quark condensate $\langle q\bar{q} \rangle / \langle q\bar{q} \rangle_V$ (4) is entirely fixed by the scalar nucleon density ρ_S (for given $\Sigma_\pi \approx 45 \text{ MeV}$). The resulting ratio is shown in Fig. 1 by the solid (red) line as a function of the energy density ϵ while the ratio of the light quark mass to its constituent mass m_q/m_q^0 is displayed by the dot-dashed (green) line which practically coincides with the ratio of the scalar condensate according to Eq. (11). We note in passing that very similar results are obtained for the parameter set ML2 which

provides a very good fit to the Dirac-Brueckner results for the nuclear equation of state from Refs. [79, 80] and is the default parameter set used presently in the PHSD. We recall that the non-linear $\sigma - \omega$ model has been often employed in the description of heavy-ion reactions at SIS energies and its parameters been determined in comparison to nuclear flow data [78].

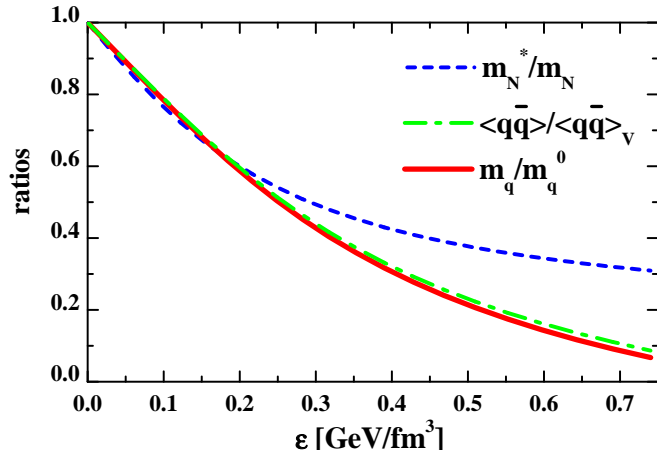


FIG. 1. The ratio m_N^*/m_N as a function of the energy density ϵ (9) at $T = 0$ in the non-linear $\sigma - \omega$ model for the parameter-set NL3 in comparison to the respective ratio for the scalar quark condensate (solid red line) from (4) (using $\Sigma_\pi = 45$ MeV). The effective light quark mass ratio m_q/m_q^0 (11) is displayed by the dot-dashed green line for comparison.

The question now arises, if there are proper experimental observables that are especially sensitive to the variation of the quark scalar condensate in a dense and hot medium. It has been suggested in Ref. [39] that when gating on central collisions of Au + Au (or Pb + Pb) such phenomena should show up in the excitation functions of suitable observables. We note that in a pure hadronic transport approach we expect a smooth behaviour of practically all observables with bombarding energy due to an increase of thermal excitation energy [81]. This is not so obvious for the PHSD approach where a gradual transition from hadronic excitations to strings and to partonic degrees-of-freedom is involved. We will argue that the strangeness ratios K^+/π^+ , K^-/π^- etc. are suitable candidates (see below).

F. The string decay in a hot and dense medium

We recall that for the bombarding energies of interest from 4 to 158 A GeV the dominant particle production in nucleus-nucleus reactions proceeds via string formation and decay. The formation and decay of strings in the vacuum has been investigated by decades and is described by the Schwinger mechanism of quark-antiquark pair production [67] as discussed in Section IIB. In the Schwinger formula for the strangeness fraction s/u (1) the string tension κ is determined experimentally (or by IQCD) as

well as the effective masses m_s, m_q for the dressed quarks. In line with common understanding this dressing is due to a scalar coupling to the vacuum condensate $\langle q\bar{q} \rangle_v$ which - according to the previous Subsection - vanishes with increasing baryon density and/or temperature. In first order the dressed quark masses are expected to scale with the ratio (4) as

$$m_s^* = m_s^0 + (m_s^v - m_s^0) \left| \frac{\langle q\bar{q} \rangle}{\langle q\bar{q} \rangle_v} \right|, \quad (10)$$

$$m_q^* = m_q^0 + (m_q^v - m_q^0) \left| \frac{\langle q\bar{q} \rangle}{\langle q\bar{q} \rangle_v} \right|, \quad (11)$$

using $m_s^0 \approx 100$ MeV and $m_q^0 \approx 7$ MeV for the bare quark masses. In the hadronic phase the ratio (1) increases with decreasing scalar quark condensate as long as the string tension κ remains approximately constant. In fact, IQCD results for the string tension below T_c show roughly a constant value while the string tension rapidly drops above T_c since no coherent electric color fields (strings) can be formed anymore. Accordingly, Eq. (1) no longer applies for the deconfined phase and the ratio s/u in PHSD is fixed to $\sim 1/3$ by comparison to the strangeness production at RHIC and LHC energies observed experimentally.

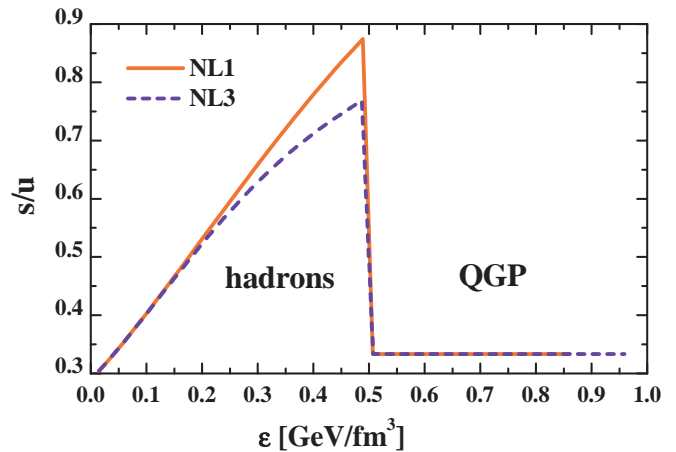


FIG. 2. The strangeness ratio s/u in the string decay (1) as a function of the energy density ϵ (9) as evaluated within the non-linear $\sigma - \omega$ model for the parameter sets NL3 and NL1 for $T = 0$ on the basis of Eqs. (10), (11) and (4).

In order to illustrate our main conjecture we show in Fig. 2 the ratio s/u as a function of the energy density ϵ at temperature $T=0$ as evaluated by Eq. (9). In this case only nucleons contribute to the scalar density in Eq. (4) and the hadronic energy density which is (apart from slight corrections due to the interaction energy) roughly given by $\epsilon \approx m_N \rho_N$, where m_N is the vacuum nucleon mass and ρ_N the nuclear density. It is seen that the ratio s/u rises with nucleon density up to $\epsilon \approx 0.5$ GeV/fm³ and drops to a value of $1/3$ in the deconfined phase in case of

the PHSD. The sensitivity to the nuclear model (NL1 versus NL3) is moderate. The set ML2 practically gives the same results as the set NL3. Accordingly, the approach to CSR occurs in the hadronic phase and should be seen experimentally for local energy densities below $\epsilon_c \approx 0.5$ GeV/fm³ since there is no more any 'string decay' in the partonic phase above ϵ_c due to the direct conversion of energy and momentum to the massive quasiparticles of the QGP.

In order to implement this scenario of 'chiral symmetry restoration' in the PHSD code we solve the gap equation (8) for each cell in space-time in order to determine the scalar nucleon density ρ_S , the scalar quark condensate by Eq. (4) and the strangeness ratio by Eq. (1) which drives the string decay in each local cell. Note that in the case of HSD (without any deconfined partonic phase) the ratio s/u increases further with energy density ϵ up to the limiting values given by bare masses $m_s = m_s^0$ and $m_q = m_q^0$ in Eq. (1). Accordingly, one has to expect an overestimation of strangeness production in the HSD when implementing CSR via (1) at high bombarding energies where the scalar quark condensate is vanishing in the overlap zone of the reaction.

We close this Section by noting that the PHSD approach has been extended to include the essential features of chiral symmetry restoration in the hadron production via the Schwinger mechanism (1). One might criticise that the value of Σ_π as well as the nuclear equation of state (NL1, ML2, NL3) are still uncertain to some extent but these 'error bars' are small compared to the leading order terms in the dynamics. Furthermore, a fully consistent approach has to include the chiral partners of 0^- and 1^- mesons, i.e. the (broad) scalar 0^+ and axial vector 1^+ mesons. Also on the baryonic side the chiral partners to the lightest baryons have to be incorporated in the transport approach with dynamical spectral functions that become identical in the chiral limit. Furthermore, the baryon propagators have to be refined in including the real and imaginary parts of the scalar and vector selfenergies also for the dynamical evolution of the system and the computation of in-medium transition rates. Since in principle the PHSD is suited for this task due to its off-shell nature we delay a self-consistent treatment of the chiral dynamics to a future more elaborate study.

III. RESULTS FOR CENTRAL AU+AU COLLISIONS FROM 4 TO 158 A GeV

We recall that numerical results for the space-time dependence of the scalar condensate ratio (4) from HSD calculations have been shown already in Figs. 3 and 4 of Ref. [81] for central Au + Au collisions at 6 A·GeV and 20 A·GeV, respectively. For an illustration we present here additionally the ratio (4) in Fig. 3 as a function of x and z (for $y = 0$) at different times t for a central Au+Au collisions at 30 A GeV. Whereas in the approach

phase the ratio drops to about $2/3$ inside the impinging nuclei (cf. Fig. 1) the scalar quark condensate practically vanishes in the full overlap phase from about 3 to 7 fm/c and regains the vacuum value only in the late expansion phase as noted before. However, for all times from contact (~ 2.5 fm/c) to about 8 fm/c the ratio of the scalar quark condensate remains far below unity, which implies that the decay of strings in the hadronic environment is modified substantially in the hot and dense medium.

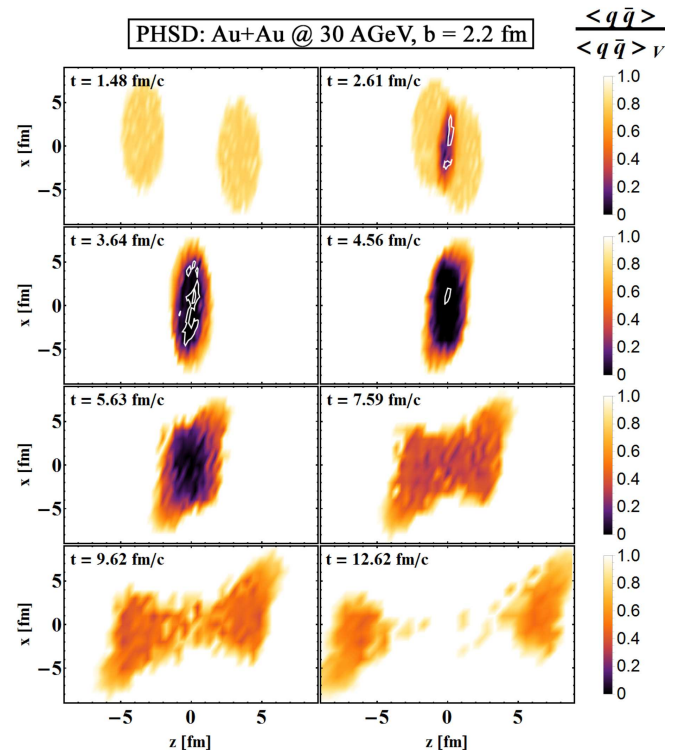


FIG. 3. The ratio (4) for the scalar quark condensate as a function of x and z (for $y = 0$) at different times t for a central Au+Au collisions at 30 A GeV employing the parameter set NL3 for the computation of the baryon scalar density. The white borderline separates the space-time regions of deconfined matter to hadronic matter.

The white borderlines in Fig. 3 separate the space-time regions of deconfined matter to hadronic matter. It is clearly seen that although the chiral symmetry is approximately restored in the full overlap phase from 2.8 to 6 fm/c some region is occupied by deconfined partons in the PHSD. In these regions, however, an enhanced production of strangeness should not occur since the Schwinger mechanism (1) no longer applies due to a vanishing string tension and a transformation of energy and momentum to massive partonic degrees-of-freedom.

After these more quantitative illustrations we continue with actual observables from heavy-ion reactions at different energies. We will consider the following four scenarios:

- The default HSD calculations without any CSR (and deconfinement transition) and a threshold in

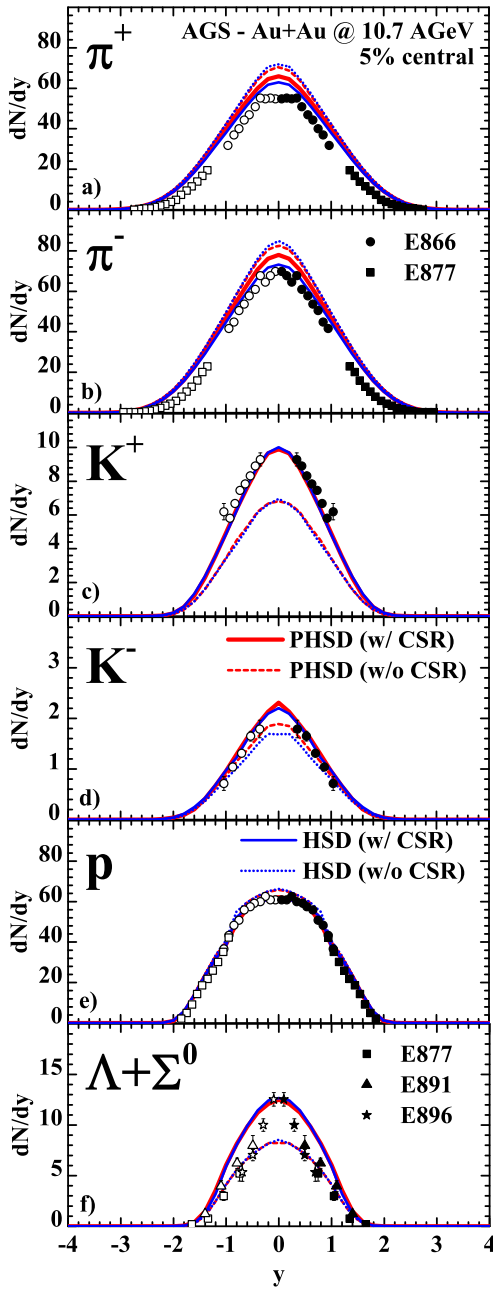


FIG. 4. The rapidity distribution of pions, kaons, protons and $(\Lambda + \Sigma^0)$'s for 5% central Au+Au collisions at 10.7 A GeV in comparison to the experimental data from Ref. [82]. The solid (red) lines show the results from PHSD (including CSR) while the blue solid lines result from HSD (including CSR) without partonic degrees-of-freedom. The dashed (red) line reflects the PHSD results without CSR while the dashed blue line results from HSD without CSR.

the local energy density of $< 0.5 \text{ GeV}/\text{fm}^3$ for elastic and inelastic reactions of formed hadrons. For energy densities above $0.5 \text{ GeV}/\text{fm}^3$ a free streaming of the particles is assumed.

- HSD calculations with the modified string decay

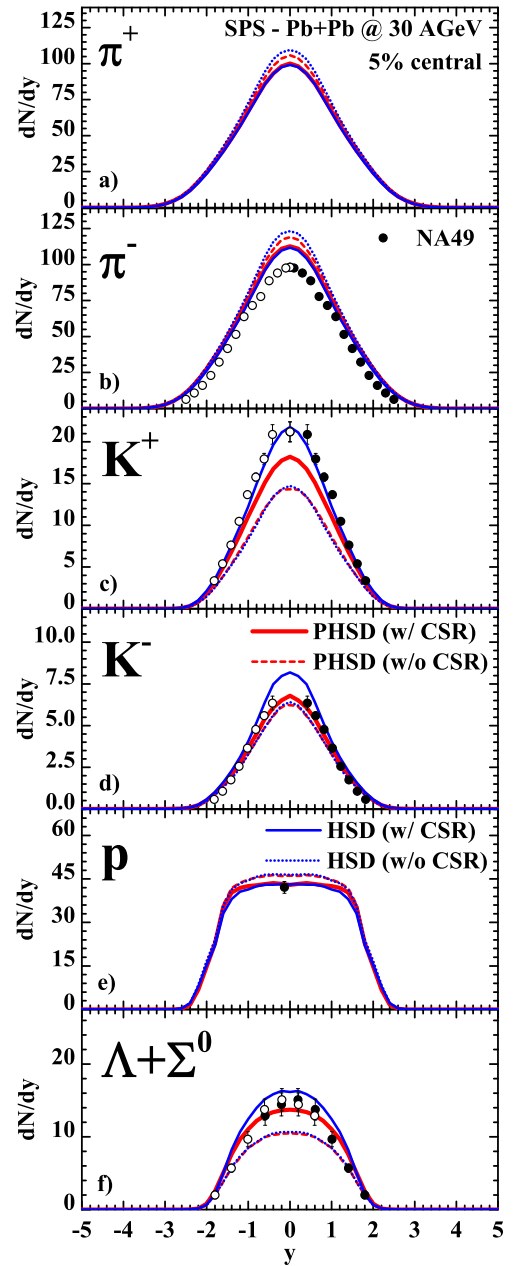


FIG. 5. The rapidity distribution of pions, kaons, protons and $(\Lambda + \Sigma^0)$'s for 5% central Pb+Pb collisions at 30 A GeV in comparison to the experimental data from Ref. [83]. The coding of the lines is the same as in Fig. 4.

(describing CSR) for all local energy densities, however, keeping the free streaming of hadrons above $0.5 \text{ GeV}/\text{fm}^3$. Also in this scenario there is no deconfinement transition.

- The default PHSD calculations without any CSR, however, a crossover transition to the deconfined phase above the threshold in the local energy density of $0.5 \text{ GeV}/\text{fm}^3$.
- PHSD calculations with the modified string de-

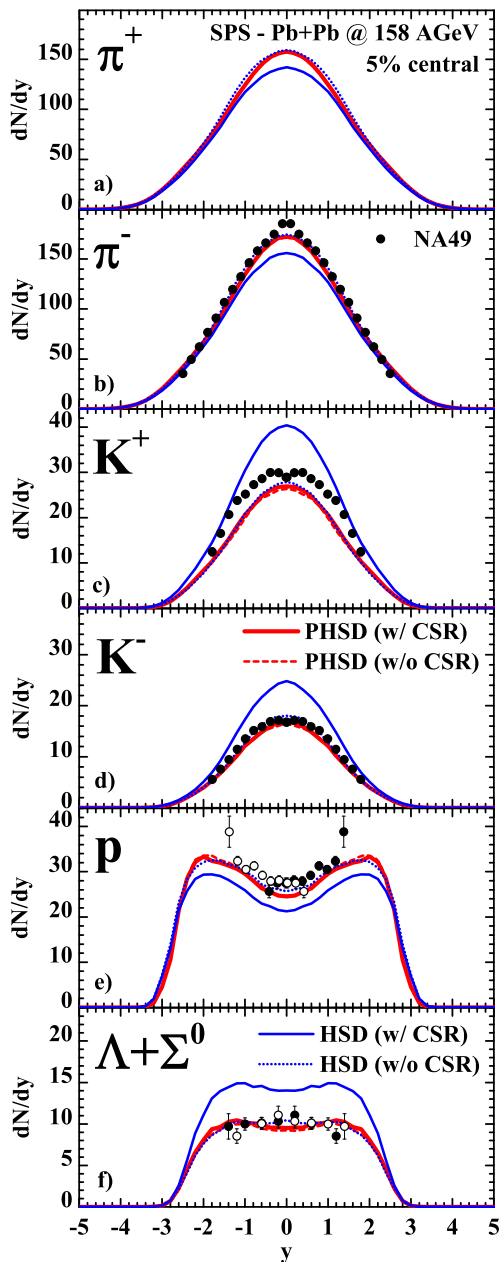


FIG. 6. The rapidity distribution of pions, kaons, protons and $(\Lambda + \Sigma^0)$'s for 5% central Au+Au collisions at 158 A GeV in comparison to the experimental data from Ref. [84]. The coding of the lines is the same as in Fig. 4.

cay (describing CSR) for energy densities below 0.5 GeV/fm³ and a crossover transition to the deconfined phase above the threshold in the local energy density of 0.5 GeV/fm³.

The results for the rapidity distributions of pions, kaons, protons and $(\Lambda + \Sigma^0)$'s in the different limits are shown in Figs. 4 to 6 for 5% central Au+Au collisions at 10.7, 30 and 158 A GeV in comparison to the experimental data from Refs. [82–84]. Here the solid (red) lines show the results from PHSD (including CSR) while the

blue solid lines result from HSD (including CSR) without partonic degrees-of-freedom. The dashed (red) line reflects the PHSD results without CSR while the dashed blue line results from HSD without CSR. As noted before, the HSD results (without CSR) for these hadrons are essentially the same than in the previous studies [37–39] and severely underestimate the K^+ and Λ production at the lower energies while overproducing pions. Furthermore, the partonic degrees-of-freedom in PHSD – including a phase transition to the QGP in case of sufficient local energy density – do not change the rapidity distributions (red dashed lines) compared to HSD at these energies. Actually this rough equivalence also holds for PHSD and HSD when including CSR (red and dashed solid lines) at 10.7 A GeV, however, in this case the K^\pm and $(\Lambda + \Sigma^0)$ distributions are better in line with the experimental observations.

We note that our 'HSD' results are up to 10% lower than those from Refs. [38, 39]. As discussed in section II.C. this is essentially due to a reduction of the critical energy density from 1 GeV/fm³ to 0.5 GeV/fm³ according to more recent lattice QCD results on the critical temperature T_c for 2+1 flavors [2]. This reduces the hadronic scattering rate since hadrons in local cells with energy densities above 0.5 GeV/fm³ are freely streaming.

Although the π^\pm multiplicities are still overestimated by the PHSD calculations (including CSR) at 10.7 and 30 A GeV a striking improvement is obtained with respect to the strangeness production at these energies for central Au+Au collisions. Since this result emerges without any fine-tuning of the nuclear equation of state (parameter-sets NL1, ML2, NL3) we attribute the strangeness enhancement seen in these reactions to the approximate restoration of chiral symmetry at high baryon density. This interpretation is in contrast to the early expectation in Refs. [33, 35, 36] that the enhancement of strangeness should be attributed to the formation of deconfined matter.

In order to summarize our findings we show the ratios K^+/π^+ , K^-/π^- and $(\Lambda + \Sigma^0)/\pi^-$ at midrapidity from 5% central Au+Au collisions in Fig. 7 as a function of the invariant energy $\sqrt{s_{NN}}$ up to the top RHIC energy in comparison to the experimental data available [85]. As before the solid (red) lines show the results from PHSD (including CSR) while the blue solid lines result from HSD (including CSR) without partonic degrees-of-freedom. The dashed (red) line reflects the PHSD results without CSR while the dashed blue line results from HSD without CSR. It is clearly seen from Fig. 7 that the results from HSD and PHSD merge for $\sqrt{s_{NN}} < 6$ GeV and fail to describe the data in the conventional scenario without incorporating the CSR as described in Section II (and been found earlier in Refs. [38, 39]). Especially the rise of the K^+/π^+ ratio at low bombarding follows closely the experimental excitation function when incorporating 'chiral symmetry restoration'. However, the drop in this ratio again is due to deconfinement since there is no longer any string decay in a hadronic medium at higher

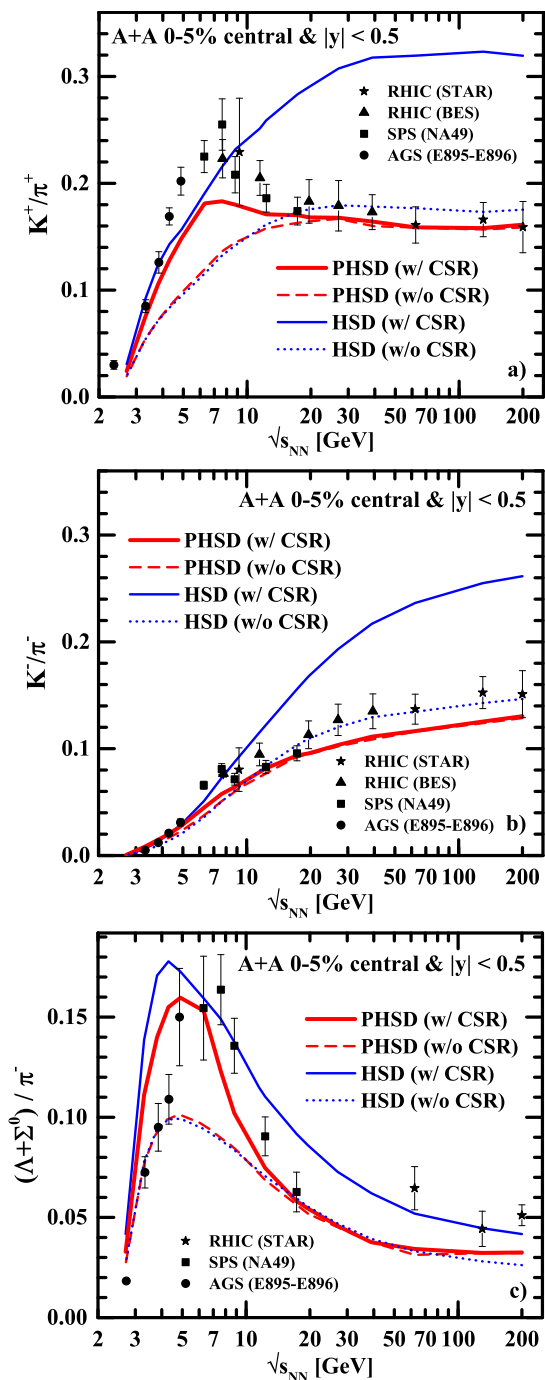


FIG. 7. The ratios K^+/π^+ , K^-/π^- (a) and Λ/π^- (b) at midrapidity from 5% central Au+Au collisions as a function of the invariant energy $\sqrt{s_{NN}}$ up to the top RHIC energy in comparison to the experimental data from [85]. The coding of the lines is the same as in Fig. 4.

bombarding energies. This is clearly seen in the case of HSD (with CSR) which overshoots the data substantially at high bombarding energy.

Accordingly the experimental 'horn' in the excitation function is caused by chiral symmetry restoration but also deconfinement is essential to observe a maximum in

the K^+/π^+ ratio. We mention that the maximum in the K^+/π^+ ratio is not so pronounced in the PHSD calculations as in the data since the pion production is still overestimated by the PHSD. We speculate that this overestimation might be due to the complex pion dynamics in the nuclear medium where the pion separates into a 'pion' and ' Δ -hole' branch [86].

IV. SUMMARY

We have studied effects from chiral symmetry restoration (CSR) in relativistic heavy-ion collisions in the energy range from 4 to 158 A GeV by using the Parton-Hadron-String Dynamics (PHSD) approach [53] that has been extended essentially in the hadronic phase to also describe CSR apart from a deconfinement transition to dynamical quarks, antiquarks and gluons in the QGP.

We have assumed that effects of chiral symmetry restoration for the scalar quark condensate $\langle q\bar{q} \rangle$ in the hadronic medium show up in the Schwinger formula (1) for the s/u ratio when the string decays in a dense or hot hadronic medium. The evaluation of the scalar quark condensate has been based on Eq. (4) where dominantly the quantity $\Sigma_\pi \approx 45$ MeV enters as well as the scalar nucleon density ρ_S that drives CSR at low temperatures of the system. Although the value of Σ_π might be slightly different [72, 73] we have kept this conservative value for our studies. The computation of the scalar baryon density $\rho_S(\mathbf{r}; t)$ has been based on the nonlinear $\sigma - \omega$ model for nuclear matter [77, 78] and in particular on the gap equation (8) for each cell of the space-time grid employing different parameter-sets. These equations complete the description of the extended PHSD approach. We note in passing that we just have used 'default values' for the couplings and low-energy constants and not attempted to perform any fitting.

When comparing the results from the extended PHSD approach for the ratios K^+/π^+ , K^-/π^- and $(\Lambda + \Sigma^0)/\pi^-$ from the different scenarios we find from Fig. 7 that the results from HSD and PHSD merge for $\sqrt{s_{NN}} < 6$ GeV and fail to describe the data in the conventional scenario without incorporating the CSR as described in Section II. Especially the rise of the K^+/π^+ ratio at low bombarding follows closely the experimental excitation function when including 'chiral symmetry restoration' in the string decay. However, the drop in this ratio again is due to 'deconfinement' since there is no longer any hadronic string decay in a partonic medium at higher bombarding energies. This is clearly seen in the case of HSD (with CSR) which overshoots the data substantially at high bombarding energy. Accordingly the experimental 'horn' in the excitation function is caused by chiral symmetry restoration but also deconfinement is essential to observe a maximum in the K^+/π^+ and Λ/π^- ratios. The maximum in the PHSD calculations is not very pronounced since the pion abundance is still overestimated in this energy range. Our interpretation differs from the early

expectation in Refs. [33, 35, 36] that the enhancement of strangeness should be attributed to the formation of deconfined matter. Our studies thus support the conjecture of 'quarkyonic matter' [45] out-of-equilibrium in central heavy-ion collisions from about 5 to 40 A GeV.

We finally recall that a fully consistent approach has to include not only the chiral effects on the hadron production but also the chiral partners of the 0^- and 1^- mesons, i.e. the (broad) scalar 0^+ and axial vector 1^+ mesons with their spectral functions. Also on the baryonic side the chiral partners to the lightest baryons have to be incorporated in the transport approach with dynamical spectral functions that become identical in the chiral limit. Since the PHSD approach is suited for

this task due to its off-shell nature for all degrees-of-freedom we delay a selfconsistent treatment of the chiral dynamics to a future more elaborate study.

ACKNOWLEDGEMENTS

The authors acknowledge inspiring discussions with J. Aichelin, D. Cabrera, V. P. Konchakovski, O. Linnyk, R. Stock and V. D. Toneev. This work was in part supported by BMBF. The computational resources have been provided by the LOEWE-CSC as well as the SKYLLA cluster at the Univ. of Giessen.

-
- [1] Y. Aoki *et al.*, Phys. Lett. B **643**, 46 (2006).
 [2] S. Borsanyi *et al.*, JHEP **1009**, 073 (2010); JHEP **1011**, 077 (2010); JHEP **1208**, 126 (2012).
 [3] S. Borsanyi *et al.*, Phys. Lett B **730**, 99 (2014); Phys. Rev. D **92**, 014505 (2015).
 [4] P. Petreczky [HotQCD Collaboration], PoS LATTICE **2012**, 069 (2012); AIP Conf. Proc. **1520**, 103 (2013).
 [5] H.-T. Ding, F. Karsch, S. Mukherjee, arXiv:1504.05274
 [6] A. Bazavov *et al.*, Phys. Rev. D **90**, 094503 (2014).
 [7] Proceedings of Quark Matter-2014, Nucl. Phys. A **931**, 1 (2014).
 [8] P. Senger *et al.*, Lect. Notes Phys. **814**, 681 (2011).
 [9] C. S. Fischer, J. Luecker, and C. Welzbacher, Phys. Rev. D **90**, 034022 (2014).
 [10] C. S. Fischer, L. Fister, J. Luecker, and J. M. Pawłowski, Phys. Lett. B **732**, 273 (2014).
 [11] T. K. Herbst, J. M. Pawłowski, and B.-J. Schaefer, Phys. Rev. D **88**, 014007 (2013).
 [12] U. Vogl and W. Weise, Prog. Part. Nucl. Phys. **27**, 195 (1991).
 [13] M. C. Birse, J. Phys. G **20**, 1537 (1994).
 [14] V. Koch, Int. J. Mod. Phys. E **6**, 203 (1997).
 [15] J. V. Steele, H. Yamagishi, and I. Zahed, Phys. Lett. B **384**, 255 (1996); Phys. Rev. D **56**, 5605 (1997).
 [16] G. E. Brown, Prog. Theor. Phys. **91**, 85 (1987).
 [17] G. E. Brown, C. M. Ko, Z. G. Wu, and L. H. Xia, Phys. Rev. C **43**, 1881 (1991).
 [18] V. Koch and G. E. Brown, Nucl. Phys. A **560**, 345 (1993).
 [19] H. Stöcker and W. Greiner, Phys. Rep. **137**, 277 (1986).
 [20] G. F. Bertsch and S. Das Gupta, Phys. Rep. **160**, 189 (1988).
 [21] W. Cassing, V. Metag, U. Mosel, and K. Niita, Phys. Rep. **188**, 363 (1990).
 [22] C. Hartnack *et al.*, Eur. Phys. J. A **1**, 151 (1998).
 [23] W. Cassing and E. L. Bratkovskaya, Phys. Rep. **308**, 65 (1999).
 [24] C. M. Ko and G. Q. Li, J. Phys. G **22**, 1673 (1996).
 [25] S. A. Bass *et al.*, M. Belkacem, M. Bleicher, M. Brandstetter, L. Bravina, C. Ernst, L. Gerland, M. Hofmann, S. Hofmann, J. Konopka, G. Mao, L. Neise, S. Soff, C. Spieles, H. Weber, L. A. Winckelmann, H. Stöcker, W. Greiner, Ch. Hartnack, J. Aichelin, and N. Amelin, Prog. Part. Nucl. Phys. **42**, 279 (1998).
 [26] C. Hartnack, H. Oeschler, Y. Leifels, E. L. Bratkovskaya, and J. Aichelin, Phys. Rept. **510**, 119 (2012).
 [27] R. Marty and J. Aichelin, Phys. Rev. C **87**, 034912 (2013); R. Marty *et al.*, Phys. Rev. C **92**, 015201 (2015).
 [28] W. Botermans and R. Malfliet, Phys. Rep. **198**, 115 (1990).
 [29] R. Malfliet, Prog. Part. Nucl. Phys. **21**, 207 (1988).
 [30] A. Faessler, Prog. Part. Nucl. Phys. **30**, 229 (1993).
 [31] L. Tolós, A. Ramos, and A. Polls, Phys. Rev. C **65**, 054907 (2002).
 [32] W. Cassing, L. Tolós, E. L. Bratkovskaya, and A. Ramos, Nucl. Phys. A **727**, 59 (2003).
 [33] J. Rafelski and B. Müller, Phys. Rev. Lett. **48**, 1066 (1982).
 [34] R. Stock, J. Phys. G **28**, 1517 (2002).
 [35] M. Gazdzicki and M. I. Gorenstein, Acta Phys. Polon. B **30**, 2705 (1999).
 [36] M. Gazdzicki, M. Gorenstein and P. Seyboth, Acta Phys. Polon. B **42**, 307 (2011).
 [37] J. Geiss, W. Cassing, and C. Greiner, Nucl. Phys. A **644**, 107 (1998).
 [38] E. L. Bratkovskaya *et al.*, Phys. Rev. C **69**, 054907 (2004).
 [39] H. Weber, E. L. Bratkovskaya, W. Cassing, and H. Stöcker, Phys. Rev. C **67**, 014904 (2003).
 [40] H. Petersen *et al.*, Phys. Rev. C **78**, 044901 (2008).
 [41] Yu. B. Ivanov, V. N. Russkikh, and V.D. Toneev, Phys. Rev. C **73**, 044904 (2006); Yu. B. Ivanov and D. Blaschke, Phys. Rev. C **92**, 024916 (2015).
 [42] A. Andronic, P. Braun-Munzinger and J. Stachel, Nucl. Phys. A **772**, 167 (2006); Phys. Lett. B **673**, 142 (2009).
 [43] E. L. Bratkovskaya, W. Cassing, C. Greiner, M. Effenberger, U. Mosel, and A. Sibirtsev, Nucl. Phys. A **675**, 661 (2000).
 [44] V. Ozvenchuk, O. Linnyk, M.I. Gorenstein, E. L. Bratkovskaya, and W. Cassing, Phys. Rev. C **87**, 024901 (2013).
 [45] L. McLerran and R. D. Pisarski, Nucl. Phys. A **796**, 83 (2007).
 [46] A. Andronic *et al.*, Nucl. Phys. A **837**, 65 (2010).
 [47] K. Fukushima and C. Sasaki, Prog. Part. Nucl. Phys. **72**, 99 (2013).
 [48] Y. Nambu and G. Jona-Lasinio, Phys. Rev. **122**, 345 (1961).

- [49] S. P. Klevansky, *Rev. Mod. Phys.* **64**, 649 (1992).
- [50] R. Marty *et al.*, *Phys. Rev. C* **88**, 045204 (2013).
- [51] J. M. Torres-Rincon, B. Sintès, and J. Aichelin, *Phys. Rev. C* **91**, 065206 (2015).
- [52] W. Cassing and E.L. Bratkovskaya, *Nucl. Phys. A* **831**, 215 (2009).
- [53] E. L. Bratkovskaya, W. Cassing, V. P. Konchakovski and O. Linnyk, *Nucl. Phys. A* **856**, 162 (2011).
- [54] V. P. Konchakovski *et al.*, *Phys. Rev. C* **85**, 044922 (2012); *Phys. Rev. C* **85**, 011902 (2012).
- [55] O. Linnyk *et al.*, *Phys. Rev. C* **89**, 034908 (2014); *Phys. Rev. C* **88**, 034904 (2013); *Phys. Rev. C* **87**, 014905 (2013); *Phys. Rev. C* **85**, 024910 (2012); *Phys. Rev. C* **84**, 054917 (2011); *Nucl. Phys. A* **855**, 273 (2011).
- [56] T. Song, H. Berrehrah, D. Cabrera, J. M. Torres-Rincon, L. Tolos, W. Cassing, and E. L. Bratkovskaya, *Phys. Rev. C* **92**, 014910 (2015).
- [57] V. P. Konchakovski, W. Cassing, Yu. B. Ivanov, and V.D. Toneev, *Phys. Rev. C* **90**, 014903 (2014).
- [58] E. L. Bratkovskaya, S. Soff, H. Stöcker, M. van Leeuwen, W. Cassing, *Phys. Rev. Lett.* **92**, 032302 (2004).
- [59] L. P. Kadanoff and G. Baym, *Quantum Statistical Mechanics*, Benjamin, New York, 1962.
- [60] S. Juchem, W. Cassing, and C. Greiner, *Phys. Rev. D* **69**, 025006 (2004); *Nucl. Phys. A* **743**, 92 (2004).
- [61] W. Cassing, *Eur. Phys. J. ST* **168**, 3 (2009); *Nucl. Phys. A* **795**, 70 (2007).
- [62] V. Ozvenchuk, O. Linnyk, M.I. Gorenstein, E.L. Bratkovskaya and W. Cassing, *Phys. Rev. C* **87**, 064903 (2013).
- [63] W. Cassing, O. Linnyk, T. Steinert, and V. Ozvenchuk, *Phys. Rev. Lett.* **110**, 182301 (2013); T. Steinert and W. Cassing, *Phys. Rev. C* **89**, 035203 (2014).
- [64] B. Nilsson-Almqvist and E. Stenlund, *Comp. Phys. Comm.* **43**, 387 (1987); B. Andersson, G. Gustafson, and H. Pi, *Z. Phys. C* **57**, 485 (1993).
- [65] T. Sjostrand, S. Mrenna and P. Z. Skands, *JHEP* **0605**, 026 (2006).
- [66] V. Konchakovski, W. Cassing and V. D. Toneev, *J. Phys. G* **42**, 055106 (2015); *J. Phys. G* **41**, 105004 (2014).
- [67] J. Schwinger, *Phys. Rev.* **83**, 664 (1951).
- [68] W. Cassing, *Nucl. Phys. A* **700**, 618 (2002).
- [69] C. H. Li and C. M. Ko, *Nucl. Phys. A* **712**, 110 (2002).
- [70] F. Li, L. W. Chen and C. M. Ko, *Phys. Rev. C* **85**, 064902 (2012).
- [71] V. Flaminio, W. G. Moorhead, D. R. O. Morrison, and N. Rivoire, *CERN-HERA-83-02*.
- [72] M. Hoferichter, J. Ruiz de Elvira, B. Kubis, and U.-G. Meissner, arXiv:1506.04142
- [73] A. Sternbeck, to be published.
- [74] B. Friman, W. Nörenberg and V. D. Toneev, *Eur. Phys. J. A* **3**, 165 (1998).
- [75] M. Bando, T. Kugo and K. Yamawaki, *Phys. Rep.* **164**, 217 (1988).
- [76] T. D. Cohen, R. J. Furnstahl, D. K. Griegel, and X. Jin, *Prog. Part. Nucl. Phys.* **35**, 221 (1995).
- [77] J. Boguta and A. R. Bodmer, *Nucl. Phys. A* **292**, 413 (1977).
- [78] A. Lang *et al.*, *Z. Phys. A* **340**, 287 (1991).
- [79] F. de Jong and R. Malfliet, *Phys. Rev. C* **44**, 998 (1991).
- [80] F. de Jong, B. ter Haar, and R. Malfliet, *Phys. Lett. B* **220**, 485 (1989).
- [81] W. Cassing, E. L. Bratkovskaya, and S. Juchem, *Nucl. Phys. A* **674**, 249 (2000).
- [82] J. Stachel, *Nucl. Phys. A* **610**, 509C (1996); S. Albergo *et al.*, *Phys. Rev. Lett.* **88**, 062301 (2002).
- [83] C. Alt *et al.* [NA49 Collaboration], *Phys. Rev. C* **77**, 024903 (2008); C. Alt *et al.* [NA49 Collaboration], *Phys. Rev. C* **73**, 044910 (2006); C. Alt *et al.* [NA49 Collaboration], *Phys. Rev. C* **78**, 034918 (2008).
- [84] S. V. Afanasiev *et al.* [NA49 Collaboration], *Phys. Rev. C* **66**, 054902 (2002); T. Anticic *et al.* [NA49 Collaboration], *Phys. Rev. C* **83**, 014901 (2011); T. Anticic *et al.* [NA49 Collaboration], *Phys. Rev. Lett.* **93**, 022302 (2004).
- [85] B. I. Abelev *et al.* [STAR Collaboration], *Phys. Rev. C* **81**, 024911 (2010); M. M. Aggarwal *et al.* [STAR Collaboration], *Phys. Rev. C* **83**, 024901 (2011).
- [86] W. Ehehalt, W. Cassing, A. Engel, U. Mosel, and G. Wolf, *Phys. Lett. B* **298**, 31 (1993).